Orientation effects in the stopping of slow dimers in an electron gas

1993 J. Phys.: Condens. Matter 5 3289

(http://iopscience.iop.org/0953-8984/5/19/024)

J. Phys.: Condens. Matter 5 (1993) 3289–3302. Printed in the UK

Orientation effects in the stopping of slow dimers in an electron gas

Herbert M Urbassek†§, Veit Dröge† and Risto M Nieminen‡
† Institut für Theoretische Physik, Technische Universität, W-3300 Braunschweig, Germany
‡ Laboratory of Physics, Helsinki University of Technology, SF-02150 Espoo, Finland

Received 10 August 1992

Abstract. We present a theoretical study on the stopping of slow homonuclear dimers in an electron gas. Rigorous formulae are presented which express the stopping in terms of the elastic scattering cross section of the electrons off the electron–dimer potential. Explicit results are derived for potentials that allow separation of the Schrödinger equation in ellipsoidal coordinates; these express the stopping power immediately in terms of the phase shifts. The results are evaluated for a model potential, with emphasis on orientation effects in dimer stopping. For small electron gas densities, dimers aligned with their direction of flight are stopped most strongly; this effect is related to the focusing of electrons towards the dimer axis. For high electron gas densities, dimers oriented perpendicular to the flight direction are stopped most strongly, since they offer the largest cross section for large momentum transfer cross collisions.

1. Introduction

For more than a decade, the stopping of fast dimers penetrating thin foils has been investigated experimentally [1–4] and theoretically [5–7]. In more recent experiments, the electron emission accompanying the penetration of dimers through thin foils could be detected in coincidence with the dimer orientation [8]; here, a considerably larger electron yield was found for dimers aligned in the beam direction than for those aligned perpendicular to the beam. The theoretical investigation of these phenomena assumes that the stopping of the dimer is predominantly due to the interaction with the electron gas in the foil. Collisions with the nuclei of the atoms of the foil are disregarded, even though they are doubtlessly of some importance, in particular at low velocities. At high velocities ($v \gtrsim 1$ in atomic units), however, the penetrating projectile forms a dynamical *wake* in the electron gas with which the electrons interact [9].

Recent theoretical approaches to the problem of dimer stopping [10, 11] model the electron–dimer interaction as a linear superposition of two unperturbed electron–atom potentials, and use the Born series to calculate the scattering characteristics. This approach appears viable as long as the individual electron–atom potentials do not overlap, i.e. at sufficiently large interatomic separations and electron energies. In the present paper, we shall consider the opposite situation of strong overlap, where the electron can be assumed to scatter off the molecule as a whole. This situation will generally be realized at smaller electron energies and internuclear distances.

In this paper, we wish to study the stopping of homonuclear dimers in an electron gas under the assumption that the electron Fermi velocity, v_F, is large compared to the dimer

§ Permanent address: Fachbereich Physik, Universität, Postfach 3049, D-6750 Kaiserslautern, Federal Republic of Germany.

0953-8984/93/193289+14$07.50

velocity. Under this condition, it can be assumed that the stopping of the dimer is due to the elastic scattering of the electron gas electrons off the fixed electron–dimer potential; inelastic effects can be disregarded. We shall be able to present explicit results, if the form of the potential allows the Schrödinger equation to separate in prolate ellipsoidal coordinates. This method has been used by Eu and Sink to study scattering off a hard ellipsoid [12] and by Li for the continuum (scattering) states of H_2^+ [13]. The same coordinate system was employed by a number of researchers to simplify the scattering calculations in electron–molecule collisions, even though a non-separable potential was used [14–19]. By employing the method of phase shifts, we shall be able to give exact solutions. Explicit results shall be presented for the case of a model potential.

2. Dimer stopping: general formalism

Following [20], which dealt with atom stopping, we consider a dimer moving with fixed velocity $\boldsymbol{v} = (v, \boldsymbol{e})$ through an electron gas. Here, v denotes the magnitude of $\boldsymbol{v}$, and $\boldsymbol{e}$ its direction. The electron gas is macroscopically at rest; the individual electron velocities $\boldsymbol{u}$ obey a Fermi distribution

$$f(\boldsymbol{u}) = \left(3n/4\pi {v_F}^3\right) \Theta(v_F - u). \tag{1}$$

Here $n = \int \mathrm{d}^3u\, f(\boldsymbol{u})$ is the density of the electron gas, v_F is the Fermi velocity, and $\Theta(x)$ denotes the Heaviside step function. Often, instead of n or v_F, the one-electron radius r_s is used to characterize the electron gas:

$$n = 3/4\pi {r_s}^3. \tag{2}$$

We wish to calculate the total force $\boldsymbol{F}$ exerted by the electron gas on the dimer. It is easiest to calculate $\boldsymbol{F}$ in the inertial frame of the dimer. In the limit of a large ratio of dimer to electron mass—which we shall assume to be given—this inertial frame coincides with the centre-of-mass system. We denote the electron velocity in this system by

$$\boldsymbol{w} = \boldsymbol{u} - \boldsymbol{v} \tag{3}$$

and the Fermi distribution is transformed to

$$g(\boldsymbol{w}) = f(\boldsymbol{u} = \boldsymbol{w} + \boldsymbol{v}) = \left(3n/4\pi {v_F}^3\right) \Theta(v_F - |\boldsymbol{w} + \boldsymbol{v}|). \tag{4}$$

In this frame, the force exerted on the dimer stems from the scattering of the electrons in the electron–dimer potential. Here, we assume the velocities $\boldsymbol{w}$ involved to be so low that inelastic collisions, i.e. excitation or ionization of dimer electrons out of states bound to the dimer, are negligible. The electron scattering can hence be treated as pure potential scattering in the electron–dimer potential; the latter needs to be calculated self-consistently in order to take into account the interaction and screening of the electrons bound to the dimer with those of the electron gas, cf section 5.1.

The flux j of electrons incident with a velocity in an interval d^3w around $\boldsymbol{w} = (w, \boldsymbol{\Omega})$ is given by

$$j = wg(\boldsymbol{w})\, \mathrm{d}^3w. \tag{5}$$

The number of electrons scattered per unit time, $\mathrm{d}N/\mathrm{d}t$, out of this flux into an interval $\mathrm{d}^2\Omega'$ around direction $\boldsymbol{\Omega}'$ is given by

$$\mathrm{d}N/\mathrm{d}t = j\sigma(w, \boldsymbol{\Omega} \to \boldsymbol{\Omega}', \boldsymbol{\Omega}_0)\mathrm{d}^2\Omega'. \tag{6}$$

For electron scattering on a dimer, the differential cross section only depends on

$$\sigma = \sigma(w, \boldsymbol{\Omega} \cdot \boldsymbol{\Omega}_0, \boldsymbol{\Omega}' \cdot \boldsymbol{\Omega}_0, \boldsymbol{\Omega} \cdot \boldsymbol{\Omega}'). \tag{7}$$

Since potential scattering is elastic, the speed after collision, w', equals w. Due to time reversal symmetry, σ is invariant under a transformation $(\Omega, \Omega') \mapsto (-\Omega', -\Omega)$, and hence

$$\sigma(w, \Omega \cdot \Omega_0, \Omega' \cdot \Omega_0, \Omega \cdot \Omega') = \sigma(w, -\Omega' \cdot \Omega_0, -\Omega \cdot \Omega_0, \Omega \cdot \Omega'). \tag{8}$$

For homonuclear dimers, a change of $\Omega_0 \mapsto -\Omega_0$ has no effect, and hence

$$\sigma(w, \Omega \cdot \Omega_0, \Omega' \cdot \Omega_0, \Omega \cdot \Omega') = \sigma(w, \Omega' \cdot \Omega_0, \Omega \cdot \Omega_0, \Omega \cdot \Omega'). \tag{9}$$

Thus the change of momentum per unit time $\Delta p/\Delta t$ of the flux of electrons considered amounts to

$$\frac{\Delta p}{\Delta t} = m(w' - w)\frac{dN}{dt} = mw(\Omega' - \Omega)\frac{dN}{dt} \tag{10}$$

where m is the electron mass. The force on the dimer F is equal to the negative of the sum over all momentum changes of the electrons impinging from all directions on the dimer. With (5), (6) and (10), we hence obtain

$$F = \int d^3w \int d^2\Omega' \, wg(w)\sigma(w, \Omega \cdot \Omega_0, \Omega' \cdot \Omega_0, \Omega \cdot \Omega')m(w - w'). \tag{11}$$

Figure 1 shows the shifted Fermi sphere in the centre-of-mass system. The Pauli principle prevents scattering into occupied states. Hence only scattering out of the states with

$$|v + w| \leqslant v_F \tag{12}$$

into unoccupied states

$$v_F \leqslant |v + w'| \tag{13}$$

is permitted. It is easily seen, however, that the latter restriction is immaterial: if we include scattering events from an occupied state w into another occupied state $w' = w\Omega'$, its contribution to the force (11)

$$wg(w)\sigma(w, \Omega \cdot \Omega_0, \Omega' \cdot \Omega_0, \Omega \cdot \Omega')m(w - w')$$

exactly cancels the reverse process $w' \to w$ by virtue of time reversal and parity symmetry (9). The contribution of every scattering event within the inner sphere of figure 1 cancels exactly with the reverse scattering event. Thus it suffices to consider scattering out of states with $w \geqslant |v_F - v|$.

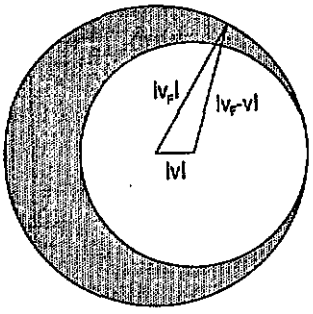

Figure 1. Schematics of the Fermi sphere (outer circle), after [20]. Since scattering preserves electron velocity in the centre-of-mass system, the Pauli principle prevents scattering out of the inner circle. Scattering processes may occur only from electron states in the grey area into unoccupied electron states outside the Fermi sphere.

It is therefore correct to omit the Pauli principle restriction on the *outgoing* states, equation (13), altogether. Integration over the *ingoing* states, however, will be restricted to the grey region of figure 1, and we have

$$F = \frac{3mn}{4\pi v_F^3} \int_{w \geqslant |v_F - v|,\ |v+w| \leqslant v_F} d^3w \, w^2 \int d^2\Omega' \, \sigma(w, \Omega \cdot \Omega_0, \Omega' \cdot \Omega_0, \Omega \cdot \Omega')(\Omega - \Omega'). \tag{14}$$

For small dimer velocities, $v \ll v_F$, the shell in which scattering occurs (the grey area in figure 1) becomes quite thin and we may approximate the condition describing the integration volume in (14) by

$$v_F - v \leqslant w \leqslant v_F - v(\Omega \cdot e) \tag{15}$$

to first order in v. In this same order, the integration over speed w may be performed in (14), yielding

$$\begin{aligned} F &= \frac{3}{4\pi} mnv_F v \int d^2\Omega \int d^2\Omega' \sigma(v_F, \Omega \cdot \Omega_0, \Omega' \cdot \Omega_0, \Omega \cdot \Omega')(1 - \Omega \cdot e)(\Omega - \Omega') \\ &= -\frac{3}{4\pi} mnv_F v \int d^2\Omega \int d^2\Omega' \sigma(v_F, \Omega \cdot \Omega_0, \Omega' \cdot \Omega_0, \Omega \cdot \Omega')\Omega \cdot e(\Omega - \Omega') \end{aligned} \tag{16}$$

where the symmetry relation (8) has been used. We may write (16) in tensorial form

$$F = -mnv_F v \hat{\sigma}(v_F) \cdot e \tag{17}$$

with the tensor

$$\hat{\sigma}(v_F) = \frac{3}{4\pi} \int d^2\Omega \int d^2\Omega' \sigma(v_F, \Omega \cdot \Omega_0, \Omega' \cdot \Omega_0, \Omega \cdot \Omega')\Omega(\Omega - \Omega'). \tag{18}$$

As is easily seen, $\hat{\sigma}$ is a symmetric positive tensor, and hence can be diagonalized. Since Ω_0 is a symmetry axis, Ω_0 and two arbitrary perpendicular axes are principal axes, with diagonal elements

$$\sigma_\parallel(v_F) = \frac{3}{4\pi} \int d^2\Omega \int d^2\Omega' \sigma(v_F, \Omega \cdot \Omega_0, \Omega' \cdot \Omega_0, \Omega \cdot \Omega')(\Omega \cdot \Omega_0)(\Omega - \Omega') \cdot \Omega_0 \tag{19}$$

$$\sigma_\perp(v_F) = \frac{3}{4\pi} \int d^2\Omega \int d^2\Omega' \sigma(v_F, \Omega \cdot \Omega_0, \Omega' \cdot \Omega_0, \Omega \cdot \Omega')(\Omega \cdot \Omega_\perp)(\Omega - \Omega') \cdot \Omega_\perp \tag{20}$$

where $\Omega_\perp \cdot \Omega_0 = 0$. The transport cross sections $\sigma_\parallel$ and $\sigma_\perp$ quantify the momentum transfer to a dimer whose orientation is aligned with its velocity, or perpendicular to its velocity, respectively.

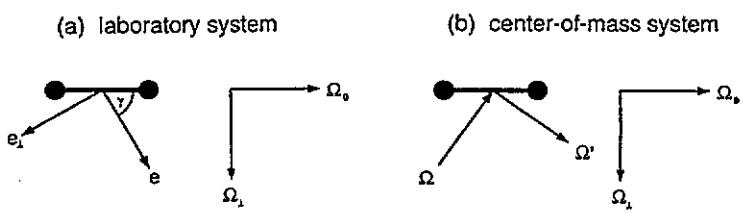

Figure 2. Relevant directions. The dimer orientation Ω_0 and the direction e of the dimer velocity define a plane, which is plotted; $\Omega_\perp$ is the direction perpendicular to Ω_0 in this plane. The angle between Ω_0 and e is γ; $e_\perp$ is the direction perpendicular to e in this plane. Ω and Ω' are the directions of an electron in the centre-of-mass system, before and after scattering on the dimer, respectively. Ω and Ω' are generally not in the plane plotted.

Let us denote the angle between e and Ω_0 by γ, cf figure 2:

$$\cos\gamma = \Omega_0 \cdot e. \tag{21}$$

We specify a direction $\Omega_\perp$ perpendicular to Ω_0 in this plane such that

$$e = \cos\gamma\,\Omega_0 + \sin\gamma\,\Omega_\perp. \tag{22}$$

Inserting this into (17), it is readily seen that

$$F = -mnv_F v[\sigma_\parallel(v_F)\cos\gamma\,\Omega_0 + \sigma_\perp(v_F)\sin\gamma\,\Omega_\perp]. \tag{23}$$

The prefactor $mnv_F v$ of the force in (23) denotes the product of electron flux nv_F on the dimer and the *net* momentum transfer mv. It is hence only the two transport cross sections that contain information on the scattering dynamics.

Equation (23) shows that generally F is not aligned with the direction of the velocity e. The component of F in the velocity direction is called the stopping power:

$$-\mathrm{d}E/\mathrm{d}x = -F\cdot e = mnv_F v[\cos^2\gamma\,\sigma_\parallel(v_F) + \sin^2\gamma\,\sigma_\perp(v_F)]. \tag{24}$$

The component perpendicular to it is given by

$$F\cdot e_\perp = mnv_F v[\sigma_\parallel(v_F) - \sigma_\perp(v_F)]\cos\gamma\sin\gamma. \tag{25}$$

It may lead to a deflection of the dimer trajectory from its straight direction e. We wish to note that the terms *stopping power* and *deflection* assume that the electron scattering only affects the centre-of-mass motion of the dimer; we thus neglect the fact that (part of) the force may excite dimer rotation and vibration. We note, however, that the *torque* on the dimer due to its interaction with the electron gas could be calculated in analogy to (14).

For a randomly oriented dimer, the stopping power amounts to

$$\left\langle -\frac{\mathrm{d}E}{\mathrm{d}x}\right\rangle = \tfrac{1}{3}mnv_F v\,\mathrm{Spur}\,\hat{\sigma}(v_F) = mnv_F v[\tfrac{1}{3}\sigma_\parallel(v_F) + \tfrac{2}{3}\sigma_\perp(v_F)] \tag{26}$$

while the deflection vanishes.

For a spherical particle, e.g. an atom, no dimer axis Ω_0 exists, and hence $\sigma = \sigma(\Omega\cdot\Omega')$ and the two transport cross sections coincide to

$$\sigma_{tr}(v_F) := \sigma_\parallel(v_F) = \sigma_\perp(v_F) = \frac{3}{4\pi}\int \mathrm{d}^2\Omega \int \mathrm{d}^2\Omega'\,\sigma(v_F, \Omega\cdot\Omega')(\Omega\cdot x)(\Omega - \Omega')\cdot x \tag{27}$$

where x may be any unit vector, or

$$\sigma_{tr}(v_F) = 2\pi\int \mathrm{d}(\Omega\cdot\Omega')\,\sigma(v_F, \Omega\cdot\Omega')(1 - \Omega\cdot\Omega') \tag{28}$$

and

$$-\frac{\mathrm{d}E}{\mathrm{d}x} = mnv_F v\sigma_{tr}(v_F). \tag{29}$$

Hence our results for a dimer coincide with the well known results [20, 21] for atom stopping, (28) and (29).

3. Scattering in ellipsoidal coordinates

In this section, we wish to calculate the scattering cross section of electrons in a potential V for the special case that the Schrödinger equation separates in ellipsoidal coordinates. From this section on, atomic units ($e^2 = \hbar = m = 1$) will be used. In the centre-of-mass system, the Schrödinger equation for the electron wavefunction Ψ is

$$\left(-\tfrac{1}{2}\Delta + V(r_1, r_2) - E\right)\Psi = 0. \tag{30}$$

Here, V is the electron–dimer interaction potential, and r_1 (r_2) measures the distance of the electron to atom 1 (2) of the dimer.

Let us assume the potential is of a special form such that (30) separates in prolate ellipsoidal coordinates $\mu = (r_1 + r_2)/R$, $\nu = (r_1 - r_2)/R$ and azimuth φ around the dimer axis; R denotes the internuclear distance of the dimer atoms. Separation of (30) leads to eigenfunctions of the form

$$\Psi_l^m(\mu, \nu, \varphi) = J_l^m(kR, \mu) S_l^m(kR, \nu) \Phi_m(\varphi) \tag{31}$$

where we indicated the dependence of the functions on the quantum numbers m and l, and on the scaled energy via the wavenumber $k = \sqrt{2E}$, explicitly. The quantum number m measures the angular momentum around the dimer axis, while l corresponds to the usual total angular momentum quantum number in the united atom limit. Note that in contrast to the spherically symmetric case, the angular eigenfunctions S_l^m, called *prolate spheroidal functions* [22], depend explicitly on energy. We use them in the normalization of Morse and Feshbach [23] (see also [24]). The radial wavefunctions satisfy

$$\left(\frac{\mathrm{d}}{\mathrm{d}\mu}(\mu^2 - 1)\frac{\mathrm{d}}{\mathrm{d}\mu} - \frac{m^2}{\mu^2 - 1} + \tfrac{1}{4}k^2R^2\mu^2 - V(\mu) - \tau_l^m\right) J_l^m(kR, \mu) = 0 \tag{32}$$

where

$$V(\mu) = 2R^2(\mu^2 - \nu^2)V(r_1, r_2) \tag{33}$$

and $\tau_l^m(kR)$ is a separation constant. We calculate S_l^m and τ_l^m using an algorithm by Press and co-workers [25]. The radial equation is solved for the boundary conditions [26]

$$J_l^m(\mu \to 1) = \text{constant} \times (\mu^2 - 1)^{m/2} \qquad J_l^m(\mu \to \infty) = 0. \tag{34}$$

We look for scattering solutions of the form

$$\Psi \sim \mathrm{e}^{\mathrm{i}k\boldsymbol{\Omega}\cdot\boldsymbol{r}} + f(kR, \boldsymbol{\Omega} \to \boldsymbol{\Omega}', \boldsymbol{\Omega}_0)\frac{2}{R\mu}\mathrm{e}^{\mathrm{i}kR\mu} \qquad \text{for } \mu \to \infty \tag{35}$$

where $\boldsymbol{\Omega}$ is the direction of the incoming electron, and f is the scattering amplitude for scattering into direction $\boldsymbol{\Omega}'$. Note that, for large μ, $\boldsymbol{\Omega} = (\nu, \varphi)$ is identical to the usual parametrization of the solid angle in terms of the cosine of the polar angle and the azimuthal angle with respect to the dimer axis. The scattering amplitude is given by

$$f(kR, \boldsymbol{\Omega} \to \boldsymbol{\Omega}', \boldsymbol{\Omega}_0) = \frac{1}{k}\sum_{m,l}\frac{2}{\Lambda_l^m} S_l^m(\nu) S_l^m(\nu') \cos m(\varphi - \varphi') \exp(\mathrm{i}\eta_l^m) \sin \eta_l^m \tag{36}$$

where the sum is over all non-negative l and $-l \leqslant m \leqslant l$, and $\Lambda_l^m(kR) = \int_{-1}^{1} \mathrm{d}\nu \left|S_l^m(kR, \nu)\right|^2$ is a normalization constant [12]. The phase shifts $\eta_l^m(kR)$ have been determined numerically from the difference of the solution of (32) with and without the potential V. The scattering cross section is then determined from the scattering amplitude by

$$\sigma(kR, \boldsymbol{\Omega} \to \boldsymbol{\Omega}', \boldsymbol{\Omega}_0) = |f(kR, \boldsymbol{\Omega} \to \boldsymbol{\Omega}', \boldsymbol{\Omega}_0)|^2. \tag{37}$$

The total scattering cross section is then given by

$$\sigma_{\mathrm{tot}}(kR, \boldsymbol{\Omega} \cdot \boldsymbol{\Omega}_0) = \int \mathrm{d}^2\boldsymbol{\Omega}' \sigma(kR, \boldsymbol{\Omega} \to \boldsymbol{\Omega}', \boldsymbol{\Omega}_0) \tag{38}$$

$$= \frac{8\pi}{k^2}\sum_{m,l}\frac{1}{\Lambda_l^m}|S_l^m(\nu)|^2 \sin^2 \eta_l^m. \tag{39}$$

In the following, we shall specify our results for a modified Yukawa potential

$$V(r_1, r_2) = Z\left(\frac{1}{r_1} + \frac{1}{r_2}\right)\exp[-\alpha(r_1 + r_2 - R)] \tag{40}$$

where Z measures the strength of the interaction, and α is a screening parameter. In the united atom limit, $R \to 0$, the potential is of pure Yukawa form, $V(r) = (2Z/r)\exp(-2\alpha r)$, where $r_1 = r_2 = r$. The factor $\exp(\alpha R)$ has been introduced in (40) in order to retain a Coulomb-like singularity of strength Z at the sites of the nuclei.

It is easily seen that only the parameters α/Z, E/Z^2 and RZ enter the problem. In the following, we shall thus specify $Z = -1$ without loss of generality. The negative value of Z characterizes the attractive interaction between the nuclei and the electrons of the electron gas.

4. Dimer stopping in ellipsoidal coordinates

The transport cross section of aligned dimers $\sigma_\parallel$, equation (19), can be calculated by substituting the cross section (37) into (19). The two azimuth integrations can be trivially performed. Figure 3 shows the resulting transport cross section when terms up to $l = 8$ are kept. We ensured that this choice is sufficient for the parameter range shown.

It is possible to calculate the transport cross sections approximately in a simple way. This can be done by approximating the spheroidal functions by their asymptotic values for small energy, $kR \to 0$:

$$S_l^m(kR, \nu) \cong P_l^m(\nu) \qquad \Lambda_l^m(kR) \cong \frac{2}{2l+1}\frac{(l+m)!}{(l-m)!} \qquad \tau_l^m \cong l(l+1). \tag{41}$$

This approximation gives

$$\sigma_\parallel(v_F) = \frac{12\pi}{k^2}\sum_{l=0}\sum_{m=-l}^{l}\frac{(l+1-m)(l+1+m)}{(2l+1)(2l+3)}\sin^2(\eta_l^m - \eta_{l+1}^m). \tag{42}$$

The comparison in figure 3 proves that this approximation is sufficiently accurate for our purposes.

Analogously, the perpendicular transport cross section evaluates to

$$\begin{aligned}\sigma_\perp(v_F) = \frac{6\pi}{k^2}\sum_{l=0}\sum_{m=0}^{l}\Bigg(&\Upsilon_m \sin^2\eta_l^m - \Upsilon_m\frac{(l+1-m)(l+1+m)}{(2l+1)(2l+3)}(\sin^2\eta_l^m + \sin^2\eta_{l+1}^m)\\ &- 2\frac{(l-m+1)(l-m+2)}{(2l+3)(2l+5)}\cos(\eta_{l+1}^{m+1} - \eta_{l+2}^m)\sin\eta_{l+1}^{m+1}\sin\eta_{l+2}^m\\ &+ 2\frac{(l+m+1)(l+m+2)}{(2l+1)(2l-1)}\cos(\eta_{l+1}^{m+1} - \eta_l^m)\sin\eta_{l+1}^{m+1}\sin\eta_l^m\Bigg)\end{aligned} \tag{43}$$

where $\Upsilon_m = 1$ for $m = 0$, and 2 otherwise.

One easily shows that for the spherical problem, i.e. if $\eta_l^m = \eta_l$ independent of m, (42) and (43) reduce to

$$\sigma_{tr} = \sigma_\parallel = \sigma_\perp = \frac{4\pi}{k^2}\sum_l (l+1)\sin^2(\eta_l - \eta_{l+1}). \tag{44}$$

This is the well known and exact result for the transport cross section for a spherically symmetric potential [21].

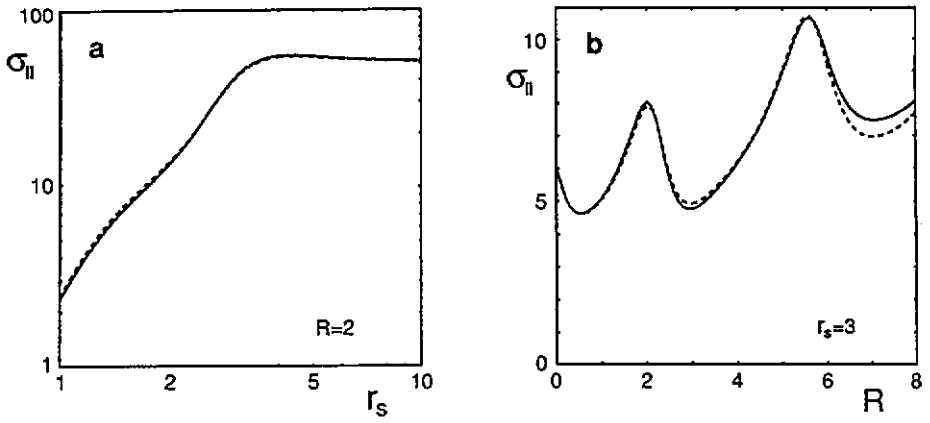

Figure 3. Comparison of the transport cross section $\sigma_{\parallel}$ of a H_2^+-dimer ($Z = -1$, $\alpha = 1$) calculated rigorously from (19) (full curve), and from the approximation (42) (broken curve). The Fermi velocity is given via the one-electron radius r_s, cf (2).

5. Results and discussion

5.1. Self-consistency

In the following, we wish to apply our results to a self-consistent dimer potential. We identify Z in (40) with the atomic charge of a dimer atom. Then the screening α is chosen according to the Friedel sum rule [21, 27, 28], which stems from the requirement that the electron gas totally screens the dimer; it essentially expresses charge neutrality. For a dimer, it is

$$Z = -\frac{1}{\pi}\sum_{m,l}\eta_l^m(v_F). \tag{45}$$

For the modified Yukawa potential (40), the Friedel sum rule can be used to fix the screening α if Z and R are given.

5.2. Stopping of dimers in an electron gas

In figure 4, we display several quantities connected with the scattering of electrons off a H_2^+ dimer in an electron gas. Figure 4(*a*) shows how the self-consistent screening α increases with increasing electron gas density. However, even for a dilute electron gas, $r_s \to \infty$, the screening does not vanish. This behaviour is reflected in the dependence of the phase shifts η_l^m against electron gas density, cf figure 4(*b*). For large r_s, all phase shifts are small except η_0^0, i.e. we have dominant s scattering. Here $\eta_0^0 \to \pi$ indicating that, for small electron gas densities, we have one (doubly occupied) bound state. This is a direct consequence of the Friedel sum rule (45). Note that for small electron gas densities, H_2^+ is therefore neutral. This is in contrast to the case of embedding a H atom in a dilute electron gas, where H^- is the stable charge state at small electron gas densities.

For increasing electron gas densities, phase shifts η_l^m with larger l values contribute, and even become dominant. In the r_s region displayed in figure 4, this applies in particular to the $l = 1$ states.

The total scattering cross section shows a distinct and interesting orientation dependence: over the whole range of electron gas densities shown, scattering on an aligned dimer is stronger than on a dimer that is oriented perpendicular to its velocity. Formally, this

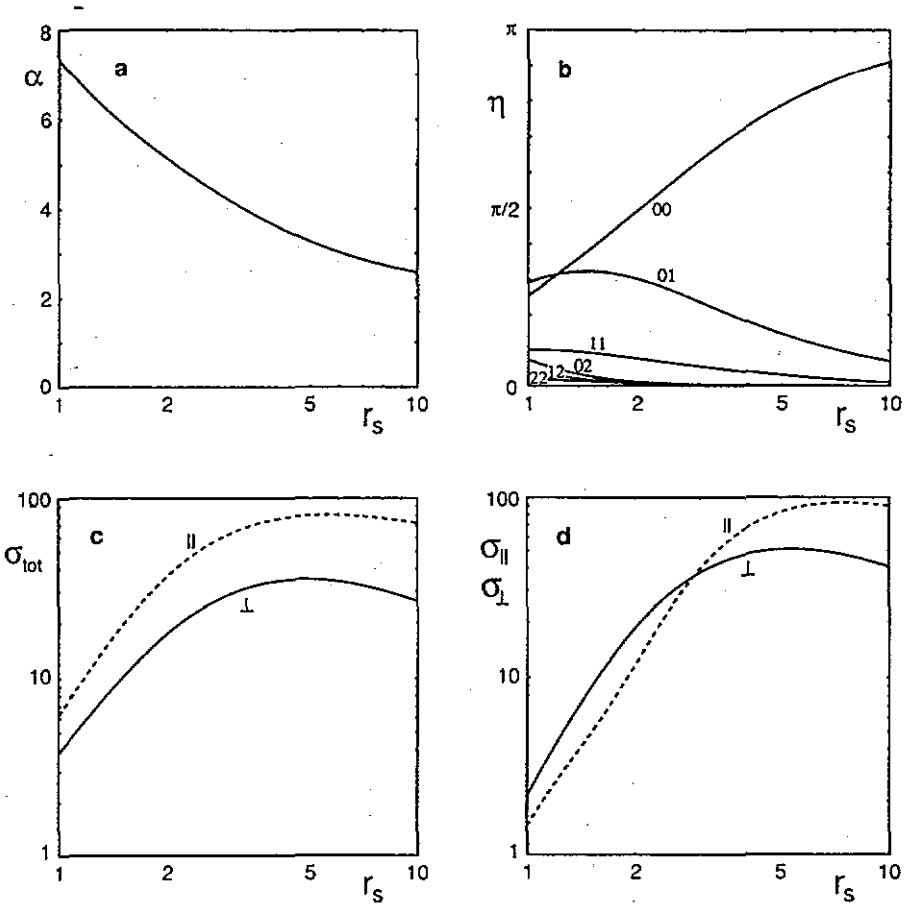

Figure 4. Self-consistent interaction of a H_2^+ dimer ($R = 2.0$) with an electron gas, as a function of the electron gas one-electron radius r_s. (*a*) Screening α determined self-consistently via the Friedel sum rule (45). (*b*) Phase shifts η_l^m. The parameters at the curves indicate the relevant values of (ml). (*c*) Total scattering cross section σ_{tot} for dimers aligned ($\|$) and perpendicular ($\perp$) to their velocity. (*d*) Transport cross section for dimers aligned ($\|$) and perpendicular ($\perp$) to their velocity.

behaviour is connected to the fact that $\sin^2 \eta_1^0 \gg \sin^2 \eta_1^1$. Since it is essentially this quantity that weighs the orientation dependence of σ_{tot} in (39), the total scattering cross section is large where $|S_1^0|$ is, i.e. at $\nu = \pm 1$, for the aligned geometry.

Intuitively, this orientation effect can be explained in a classical picture as follows. Electrons incident parallel to the dimer axis are attracted by the first atom further toward the axis and thus come close to the second atom, where they are then even more strongly scattered. The focusing effect is missing for electrons incident perpendicular to the dimer axis. This effect has recently been discussed in a more detailed way [29].

The scattering cross section has a maximum at a one-electron radius of $r_s \cong 5$; the exact value depends on the dimer orientation. It decreases towards larger r_s, since then all $\eta_l^m \to 0$ except η_0^0 which tends to π; hence, according to (39), σ_{tot} vanishes. At small r_s, on the other hand, σ_{tot} decreases. Here the region of validity of the first Born approximation starts, which predicts $\sigma_{tot} \propto 1/k^2$ for large k.

Figure 4(*d*), finally, displays the transport cross section. Its general dependence on the

one-electron radius r_s follows σ_{tot} with a maximum at $r_s = 5$–10 and a decrease towards zero for small and large electron gas densities. Its orientation dependence is more intricate, though. While at small gas densities, the aligned dimer is more strongly stopped than in the perpendicular orientation; this behaviour is reversed for $r_s < 3$. This is due to the fact that the transport cross section predominantly measures strong scattering events, i.e. large deflections $\Omega' - \Omega$, cf (18). Classically, this favours impact parameters in the vicinity of the nuclei, and hence the perpendicular orientation, since here two nuclei, rather than one, are 'visible' to the electrons. In quantum mechanics, this feature gains importance only for high electron gas densities where the relevant electron wavelength λ is sufficiently small.

Figure 5 shows total and transport cross sections of a H_2^+ dimer in a dense ($r_s = 2$) and dilute ($r_s = 5$) electron gas, as a function of internuclear separation R. The averaging of σ_{tot} has been performed numerically by integration over all molecular axes Ω_0. A prominent feature are the oscillations for $r_s = 2$ in the aligned geometry. They appear to represent a resonance condition where half the electron wavelength $\lambda/2 \cong 3.3$ coincides with the internuclear distance R. From what has been said above about the focusing effect in the aligned geometry, such a resonance is not to be expected in the perpendicular geometry. In fact, there the oscillations are considerably weaker, such that the averaged cross sections are rather smooth. For a dilute electron gas, the cross sections show a behaviour similar to the high-density case, but on an enlarged scale of internuclear distance. This is correlated to the fact that the electron wavelength increases with r_s, $\lambda \cong 3.3 r_s$.

5.3. Discussion and outlook

Available theories of dimer stopping in a homogeneous electron gas take their starting point from a superposition of two Yukawa potentials based on the atomic nuclei of the dimer

$$V(r_1, r_2) = \frac{Z}{r_1} e^{-\alpha r_1} + \frac{Z}{r_2} e^{-\alpha r_2} \tag{46}$$

where the screening constant α is calculated via the Friedel sum rule self-consistently for one *atom* in the electron gas. Stopping is calculated via first-order [5, 6] or second-order [11] Born theory. Often, only s-wave scattering on each atomic nucleus is taken into account [6], even if multiple scattering effects of electrons between the nuclei are considered [7]. Orientation dependent effects have not been rigorously discussed following this line of approach. This approach is reasonable, if scattering on each atom is not influenced by the presence of the other atom, i.e. if $R > 2/\alpha$. For atomic distances of the order $R \cong 2$, this is fulfilled for $\alpha \gtrsim 1$. Hence for realistic densities of the electron gas, this approach is at the boundary of its domain of validity.

Our approach, on the other hand, is well adapted to the case of overlapping screening, $R < 2/\alpha$. In the united atom limit, $R \to 0$, our potential is equivalent to the above, and it is still reasonable for small R. While our method of solution is valid, and converges well, also for large R, the potential becomes unsatisfactory in that case. In fact, then we do not obtain realistic separated atoms. Thus, for realistic electron gas densities, our potential is also at the limits of its domain of validity.

The numerical results presented here are therefore mainly meant as *model* calculations. The results could be improved if the scattering cross sections for a more realistic potential were at hand. As a more realistic potential the above superposition of two Yukawa potentials (46) may be used. It would be even more preferable, however, if a self-consistent calculation on the basis of density functional theory were available. Then our formalism could be applied to calculate the transport cross sections and the stopping.

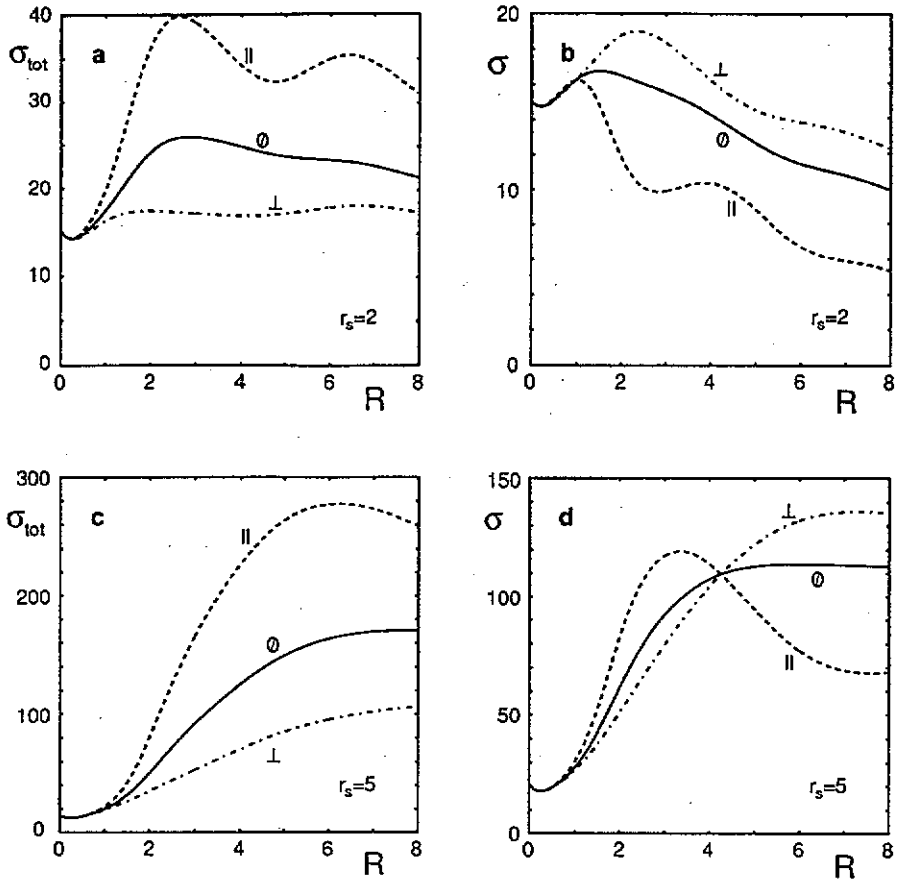

Figure 5. Self-consistent total scattering cross section (*a*), (*c*) and transport cross section (*b*), (*d*) of a H_2^+ dimer as a function of internuclear distance R, for electron gas parameters $r_s = 2$ (*a*), (*b*) and $r_s = 5$ (*c*), (*d*), for dimers aligned (∥) and perpendicular (⊥) to their velocity, and the average value for random orientation (∅).

The interaction of a slowly moving dimer with an electron gas certainly represents an interesting model problem. We mention a number of issues that have not been covered in the present work.

First, how does stopping depend on the rotational state of a dimer?

Second, molecular projectiles may dissociate while slowing down. What does this imply for the stopping power? How is the energy distributed among the constituents?

Third, and finally, dimers may become vibrationally excited by the interaction with the electron gas. This represents rather an involved issue. Low-energy electrons can scatter off a dimer resonantly so that they linger around long enough to make the dimer vibrate. The usual notion is that electrons scattering off closed-shell dimers may occupy anti-bonding orbitals and thus soften the dimer with the possibility of dissociating it. When a slow electron approaches an open-shell dimer such as H_2^+, on the other hand, it sees unoccupied bonding orbitals; then a strong scattering situation may result, in which even the Born–Oppenheimer approximation might break down. We expect, however, that these complications are not as important for a dimer screened in an electron gas as they are in the case of low-energy electrons scattering off a dimer in vacuum. Dynamic effects are smaller for the screened

dimer than for the free one, simply because in the first case the effective potential is weaker and the dimer bonding states always remain occupied.

Experimental measurements of H_2^+-ion stopping have been published for velocities $v \cong 0.7$ in C ($r_s = 1.6$) and Al ($r_s = 2.1$) foils [1,3]. The experimental data were presented in the form of the so-called vicinage function

$$g = \frac{(dE/dx)_{dimer}}{2(dE/dx)_{atom}} - 1 \tag{47}$$

which measures the relative deviation of the (orientation averaged) dimer stopping from the stopping of two isolated atoms. While the experiments measured $g = -0.1 \ldots -0.2$, our calculation predicts $g \cong +0.1 \ldots +0.2$, cf figure 6. In view of the experimental uncertainty, this discrepancy does not appear to discriminate against our approach. However, figure 6 shows that we predict strong deviations between the stopping of a H_2^+ dimer and two isolated H atoms in dilute electron gases. This is due to the above-mentioned fact that, as well as a H atom, a H_2^+ dimer binds two electrons in the electron gas. Hence a dimer interacts as a neutral entity with the electron gas, and the scattering decreases strongly with increasing electron wavelength, i.e. r_s. H atoms, on the other hand, become ionized H^- in the electron gas, and hence scatter more strongly. As a consequence, g diminishes with increasing r_s. It might be interesting to try to measure this effect by bombarding high-r_s materials with H atoms and H_2^+ dimers and measuring the difference in stopping.

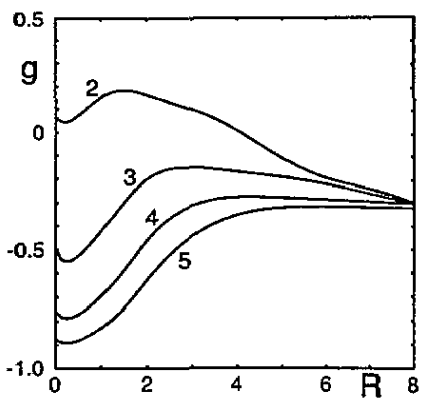

Figure 6. Vicinage function g, cf (47), of a H_2^+ dimer as a function of internuclear distance R. The curves are parametrized by the one-electron radius r_s.

At large values of R, g should go to zero. This is not the case in figure 6, and directly reflects the deficiencies of our potential (40). As discussed above, our model potential only describes scattering satisfactorily for overlapping screening $R < 2/\alpha$.

Quite recently, orientation effects in dimer stopping have been measured for higher dimer velocities, $v = 2$ [8]. These velocities are unfortunately too high to apply our formulae for the stopping power (24) directly, since these have been derived under the assumption $v \ll v_F \cong 1.9/r_s$. An evaluation of (14) that holds true for all velocities does not appear to be straightforward.

6. Summary

We presented rigorous formulae for the stopping of a homonuclear dimer in an electron gas for small velocities, $v \ll v_F$. These formulae make use of the assumption that, in the inertial frame of the dimer, stopping is due to elastic scattering of electrons off the dimer potential and that inelastic scattering, i.e. excitation or ionization of electrons bound to the dimer, can be disregarded.

These formulae were applied to potentials that allow separation of the Schrödinger equation in prolate ellipsoidal coordinates. The stopping can then be expressed in terms of the phase shifts η_l^m.

We evaluated the results for a *model* potential, with emphasis on orientation effects in dimer stopping. We showed that, at small electron gas densities, dimers flying in the direction of the dimer axis are more strongly stopped than dimers flying perpendicular to this axis. This effect can be related to the focusing of electrons toward the dimer axis. For high electron gas velocities, aligned dimers are less stopped, since they offer less cross section for central, i.e. large momentum transfer, collisions.

Our potential becomes unphysical for large internuclear distances of the dimer. It should represent reality quite well, however, for small distances. It therefore offers an approach that is complementary to that of other authors who concentrate on modelling the separated atom-limit well. We emphasize that our general formulae are valid, as long as the ellipsoidal phase shifts η_l^m can be determined from the potential.

Acknowledgments

We thank M Vicanek for discussions.

References

[1] Eckardt J C, Lantschner G, Arista N R and Baragiola R A 1978 *J. Phys. C: Solid State Phys.* **11** L851
[2] Steuer M F, Gemmell D S, Kanter E P, Johnson E A and Zabransky B J 1982 *Nucl. Instrum. Methods* **194** 277
[3] Levi-Setti R, Lam K and Fox T R 1982 *Nucl. Instrum. Methods* **194** 281
[4] Fox T R, Lam K and Levi-Setti R 1982 *Nucl. Instrum. Methods* **194** 285
[5] Arista N R 1978 *Phys. Rev.* B **18** 1
[6] Nagy I, Arnau A and Echenique P M 1990 *Nucl. Instrum. Methods* B **48** 54
[7] Barrachina R O, Calera-Rubio J and Gras-Marti A 1992 *Nucl. Instrum. Methods* B **67** 62
[8] Yamazaki Y 1991 *Interaction of Charged Particles with Solids and Surfaces (NATO ASI Series B* **271**) ed A Gras-Marti, H M Urbassek, N R. Arista and F Flores (New York: Plenum) p 423
[9] Bohr N 1948 *Mater. Fys. Meddr. Dansk. Vidensk. Selsk.* **18** No 8
[10] Pitarke J M and Echenique P M 1991 *Nucl. Instrum. Methods* B **56/57** 365
[11] Pitarke J M, Echenique P M and Ritchie R H 1991 *Nucl. Instrum. Methods* B **56/57** 369
[12] Eu B C and Sink M L 1983 *J. Chem. Phys.* **78** 4896
[13] Li M C 1972 *J. Math. Phys.* **13** 1381
[14] Stier H C 1932 *Z. Phys.* **76** 135
[15] Fisk J B 1936 *Phys. Rev.* **49** 167
[16] Nagahara S 1953 *J. Phys. Soc. Japan* **8** 165
[17] Nagahara S 1954 *J. Phys. Soc. Japan* **9** 52
[18] Massey H S W and Ridley R O 1956 *Proc. Phys. Soc.* A **69** 659
[19] Hara S 1969 *J. Phys. Soc. Japan* **27** 1009
[20] Bonderup E 1991 *Penetration of charged particles through matter* (Aarhus, Denmark: University of Aarhus) unpublished lecture notes
[21] Echenique P M and Uranga M E 1991 *Interaction of Charged Particles with Solids and Surfaces (NATO ASI Series B* **271**) ed A Gras-Marti, H M Urbassek, N R. Arista and F Flores (New York: Plenum) p 39
[22] Abramowitz M and Stegun I R 1965 *Handbook of Mathematical Functions* (New York: Dover)
[23] Morse P M and Feshbach H 1953 *Methods of Mathematical Physics* (New York: McGraw-Hill)
[24] Stratton J A, Morse P M, Chu L J, Little J D C and Corbató F J 1956 *Spheroidal Wave Functions* (New York: Wiley)
[25] Press W H, Flannery B P, Teukolsky S A and Vetterling W T 1989 *Numerical Recipes* (Cambridge: Cambridge University Press)
[26] Moores D L 1979 *Electron–Molecule and Photon–Molecule Collisions* ed T Rescigno, V McKoy and B Schneider (New York: Plenum) p 3

[27] Friedel J 1952 *Phil. Mag.* **43** 153
[28] Kittel C 1963 *Quantum Theory of Solids* (New York: Wiley)
[29] Dröge V and Urbassek H M 1992 *J. Phys. B: At. Mol. Phys.* **25** L225